

## **On the detectability of quasi-circular co-orbital planets. Application to the radial velocity technique.**

**A. Leleu (1)**, P Robutel (1) and A.C.M. Correia (2),(1)

(1) ASD, IMCCE-CNRS UMR8028, Observatoire de Paris, UPMC, 77 Av. Denfert-Rochereau, 75014 Paris, France; (2) CIDMA, Departamento de Física, Universidade de Aveiro, Campus de Santiago, 3810-193 Aveiro, Portugal (adrien.leleu@obspm.fr)

### **Abstract**

Several celestial bodies in co-orbital configurations exist in the Solar System. However, co-orbital exoplanets are yet to be discovered. This lack may result from a degeneracy between the signal induced by co-orbital planets and other orbital configurations. Here we determine a criterion for the detectability of quasi-circular co-orbital planets and develop a demodulation method to bring out their signature from the observational data. We show that the precision required to identify a pair of co-orbital planets depends only on the libration amplitude and on the planet's mass ratio. We apply our method to synthetic radial velocity data, and show that for tadpole orbits we are able to determine the inclination of the system to the line-of-sight. Our method is also valid for planets detected through the transits or astrometry techniques.

## Coorbital motion in the co-planar RTBP: family of Quasi-satellite periodic orbits

A. Pousse, P. Robutel and A. Vienne

(1) IMCCE - Observatoire de Paris, Paris, France (alexandre.pousse@obspm.fr)

### Abstract

In the framework of the Restricted Three-body Problem (RTBP), we consider a primary whose mass is equal to one, a secondary on circular or eccentric motion with a mass  $\epsilon$  and a massless third body. The three bodies are in coplanar motion and in co-orbital resonance. We actually know three classes of regular co-orbital motions: in rotating frame with the secondary, the tadpole orbits (TP) librate around Lagrangian equilibria  $L_4$  or  $L_5$ ; the horseshoe orbits (HS) encompass the three equilibrium points  $L_3$ ,  $L_4$  and  $L_5$ ; the quasi-satellite orbits (QS) are remote retrograde satellite around the secondary, but outside of its Hill sphere.

Contrarily to TP orbits which emerge from a fixed point in rotating frame, QS orbits emanate from a one-parameter family of periodic orbits, denoted family-f by Henon (1969). In the averaged problem, this family can be understood as a family of fixed points. However, the eccentricity of these orbits can reach high values. Consequently a development in eccentricity will not be efficient. Using the method developed by Nesvorný et al. (2002) which is valid for every values of eccentricity, we study the QS periodic orbits family with a numerical averaging.

In the circular case, I will present the validity domain of the average approximation and a particular orbit. Then, I will highlight an unexpected result for very high eccentricity on families of periodic orbits that originate from  $L_3$ ,  $L_4$  and  $L_5$ . Finally, I will sketch out an analytic method adapted to QS motion and exhibit associated results in the eccentric case.

## Tidal formation of Hot Jupiters in binary star systems

M. Bataille (1), A.-S. Libert (1) and A.C.M. Correia (2,3)

(1) NaXys, University of Namur, 8 Rempart de la Vierge, 5000 Namur, Belgium (manon.bataille@unamur.be, anne-sophie.libert@unamur.be), (2) Department of Physics, CIDMA, University of Aveiro, Campus Universitario de Santiago, 3810-193 Aveiro, Portugal, (3) Astronomie et Systèmes Dynamiques, IMCCE-CNRS UMR8028, Observatoire de Paris, 77 Av. Denfert-Rochereau, 75014 Paris, France

### Abstract

More than 150 Hot Jupiters with orbital periods less than 10 days have been detected. Their in-situ formation is physically unlikely. We need therefore to understand the migration of these planets from high distance (several AUs). Three main models are currently extensively studied: disk-planet interactions (e.g. [3]), planet-planet scattering (e.g. [4]) and Kozai migration (e.g. [2]). Here we focus on this last mechanism, and aim to understand which dynamical effects are the most active in the accumulation of planetary companions with low orbital periods in binary star systems.

To do so, we investigate the secular evolution of Hot Jupiters in binary star systems. Our goal is to study analytically the 3-day pile-up observed in their orbital period. Our framework is the hierarchical three-body problem, with the effects of tides, stellar oblateness, and general relativity. Both the orbital evolution and the spin evolution are considered. Using the averaged equations of motion in a vectorial formalism of [1], we have performed  $\sim 100000$  numerical simulations of well diversified three-body systems, reproducing and generalizing the numerical results of [2].

Based on a thorough analysis of the initial and final configurations of the systems, we have identified different categories of secular evolutions present in the simulations, and proposed for each one a simplified set of equations reproducing the evolution. Statistics about spin-orbit misalignments and mutual inclinations between the orbital planes of the Hot Jupiter and the star companion are also provided. Finally, we show that the extent of the 3 day pile-up is very dependent on the initial parameters of the simulations.

### Acknowledgements

This research used resources of the "Plateforme Technologique de Calcul Intensif (PTCI)" located at the

University of Namur, Belgium, which is supported by the F.R.S.-FNRS under the convention No. 2.4520.11.

### References

- [1] Correia, A. C. M., Laskar, J., Farago, F. and Boué, G.: Tidal evolution of hierarchical and inclined systems, *Celestial Mechanics and Dynamical Astronomy*, Volume 111, pp. 105-130, 2011.
- [2] Fabrycky, D. and Tremaine, S.: Shrinking Binary and Planetary Orbits by Kozai Cycles with Tidal Friction, *The Astrophysical Journal*, Volume 669, pp. 1298-1315, 2007.
- [3] Lin, D. N. C., Bodenheimer, P. and Richardson, D. C.: Orbital migration of the planetary companion of 51 Pegasi to its present location, *Nature*, Volume 380, pp. 606-607, 1996.
- [4] Nagasawa, M., Ida, S. and Bessho, T.: Formation of Hot Planets by a Combination of Planet Scattering, Tidal Circularization, and the Kozai Mechanism, *The Astrophysical Journal*, Volume 678, pp. 498-508, 2008.

## On the rotation of co-orbital bodies

**P. Robutel** (1), A. Leleu (1) and A. Correia (2,1)

(1) IMCCE, Observatoire de Paris, UPMC, CNRS UMR8028, 77 Av. Denfert-Rochereau, 75014 Paris, France,

(2) Departamento de Fisica, I3N, Universidade de Aveiro, Campus de Santiago, 3810-193 Aveiro, Portugal

### Abstract

The rotation of asymmetric bodies in eccentric Keplerian orbits may be chaotic. As it is the case for Hyperion [1], this phenomenon is due to the overlapping of spin-orbit resonances. For a Keplerian motion with small eccentricity, the only relevant spin-orbit resonance is the synchronous one (when the orbital frequency is equal to the rotation frequency as it is the case for the Moon). As a consequence, the rotation is generally regular.

Here we are interested in the rotation of a body whose orbital motion is perturbed by a third one. The situation in which the rotator and the perturbing body are in co-orbital resonance (1:1 orbital resonance) is particularly interesting. We demonstrate that, even when the eccentricities of the trajectories are small, stable non-synchronous rotation is possible for a wide range of mass ratios and body shapes [2]. We further show that the rotation becomes chaotic when the natural rotational libration frequency, due to the axial asymmetry, is of the same order of magnitude than the orbital libration frequency inside the co-orbital resonance. When the co-orbital bodies evolve on elliptic orbits with significant eccentricities, case in which non-synchronous spin-orbit resonances are possible on Keplerian orbits, a new kind of spin-orbit resonance appears.

### References

- [1] Wisdom, J. and Peale, S. J. and Mignard, F.: The chaotic rotation of Hyperion, *Icarus*, Vol. 58, pp. 137-152, 1984.
- [2] Correia, A. C. M. and Robutel, P.: Spin-orbit coupling and chaotic rotation for coorbital bodies in quasi-circular orbits, *APJ*, Vol. 779, pp. 20, 2013.

## Asteroid flux and water transport towards circumprimary habitable zones in binary star systems

**D. Bancelin** (1,2), E. Pilat-Lohinger (1), S. Eggl (2), H. Lammer (3), C. Johnston (1), T.I. Maindl (1) and R. Dvorak (1)

(1) Institute of Astrophysics, University of Vienna, Austria (david.bancelin@univie.ac.at)

(2) IMCCE, Paris Observatory, France

(3) Space Research Institute(IWF), Austrian Academy of Sciences (ÖAW), Graz, Austria

### Abstract

Dynamical simulations show that the outcome of planetary formation process can lead to various planetary architectures (i.e. location, size, mass and water content) when the star system is single or double. In the late phase of planetary formation, when embryo-sized objects dominate the inner region of the system, asteroids are also present and can provide additional material for objects inside the habitable zone (HZ). In this study, we make a comparison of several binary star systems' characteristics and their efficiency to move icy asteroids from beyond the snow-line into orbits crossing the HZ. In our results, we highlight the key role of secular and mean motion resonances, causing an efficient flux of asteroids to the HZ on a short timescale. This in turn leads to asteroids bearing a non negligible amount of water towards the HZ and available for any planets or embryos moving in this area. We also discuss how mass loss mechanisms can alter the water content on asteroids' surface.

### Introduction

Up to now, almost two thousands exoplanets are listed, not to mention the almost three thousands candidates from Kepler observations. Most of them orbit single stars, but some planets or planetary systems were found in multiple star systems. In our solar neighbourhood, almost 70% of the known systems are composed of multiple stars. The question of habitability in binaries, by taking into account the combined radiation and dynamical effects for the determination of the HZ borders, has already been studied in [1] for known systems and they conclude that both stars could harbor potential habitable planets in their respective HZ. Previous studies [2] of planetary formation from embryo-sized objects in such systems show the stochastic behaviour of the simulations on the archi-

itecture of the planetary system formed. Planets can form in the HZ but they can be dry or almost dry. However, smaller objects are also present in the feeding area, providing additional material. The main question we tackle in this study is the efficiency of a secondary star to move icy asteroids from beyond the snow-line into orbits crossing the HZ. Considering various binary star characteristics, how much water can be transported into the habitable zone and on which timescale? If mass loss processes on asteroids' surface are accounted for, how much water can really end on any planets or embryos moving in the HZ?

### Numerical simulations

Our study is focused on a primary G-type star with mass  $M_{\star} = 1 M_{\odot}$  and we investigate the dynamical effect of a secondary of either F, G, K and M-type, on an asteroid belt. The studied binary star systems encompass relatively tight configurations, i.e. semi-major axes in a range of  $a_b \in [25:100]$  au. This parameter has been changed in steps of 25 au in our simulations. The secondary is on an elliptical coplanar orbit with eccentricities  $e_b \in [0.1:0.5]$  increased in steps of 0.2. We modeled a belt of 10000 asteroids (remnants from the late phase of planetary formation process) beyond the snow line. The planetesimals are placed randomly around the primary star and move under the gravitational influence of the two stars and a gas giant placed at 5.2 au with a mass equal to Jupiter's mass.

Contrary to a single star system, the presence of a secondary star causes secular perturbations which position, for a given giant planet location, is strongly related to the binary system's characteristics. Figure 1 shows the maximum eccentricity of test particles initially on a circular coplanar orbit and placed below the orbit of the gas giant planet ( $\bullet$ ). Several scenarios are studied but only results for  $a_b = 50$  and 100 au

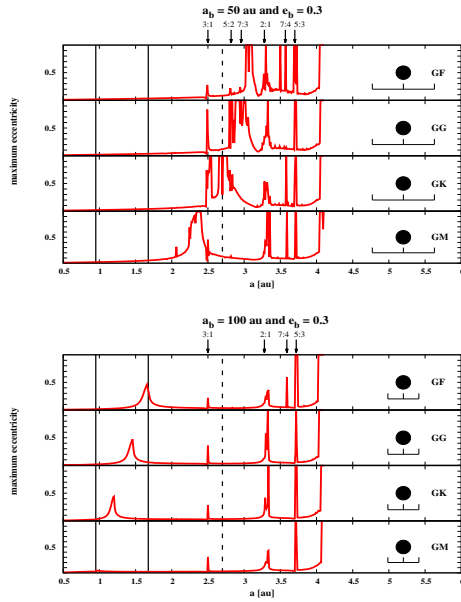


Figure 1: Maximum eccentricity of test particles initially placed on a circular-plan orbit, below the giant planet (●) at 5.2 au. In both cases, the secondary is on an elliptical coplanar orbit. *Bottom panel*: the secondary is at  $a_b = 100$  au. When varying the secondary's mass, MMRs can become stronger and the secular perturbation inside the HZ (straight vertical lines) moves outward. *Top panel*: the secondary is at  $a_b = 50$  au. The secular perturbation exhibits the same behaviour, however it reaches the icy asteroid belt region, located after the snow-line at 2.7 au (dashed line).

are shown for a fixed value  $e_b = 0.3$ . We can clearly identify, for the case of  $a_b = 100$  au, the perturbed area moving outward for increasing secondary's mass. For this particular case, the secular perturbation lies inside the HZ (straight lines). When decreasing  $a_b$ , this secular perturbation moves outward and can reach the asteroid belt region, located after the snow-line at 2.7 au (dashed vertical line). For this case, the secular perturbation overlaps with the mean motion resonances (MMRs) whereas objects inside the HZ move on quasi-circular orbit.

In our results, we highlight the key role of secular perturbation and MMRs and we analyse the consequences of such dynamics on:

- the stability of asteroids in such binary systems i.e. their lifetime and dynamical outcome
- the transport of water to the HZ

- the probability for an asteroid to deliver its water content to any planets or embryos moving in the HZ

We show that binary star systems can produce a more efficient flux of asteroids to the HZ on a short timescale. This in turn leads to asteroids bearing a non negligible amount of water to the HZ compare to single star systems. However, mass loss mechanisms such as ice sublimation, collision and strong XUVs from a younger primary star, can alter the water content on asteroids' surface. We discuss the consequences for water delivery to planets or embryos inside the HZ.

## Conclusion

We show in our study how different is the dynamics in single and binary star systems when including a giant planet: the asteroid flux and water transport is boosted by the strength of secular and mean motion resonances in binary star systems. Indeed, asteroids increase their eccentricity much faster and can rapidly reach the HZ region. This implies additional water sources in the HZ. However, mass loss processes can drastically decrease the amount of water beared to the HZ.

## Acknowledgements

DB, EPL, TM, RD, HL and CJ acknowledge the support of the FWF NFN project: "Pathways to Habitability" and related subprojects respectively S11608-N16 "Binary Star Systems and Habitability", S11603-N16 "Water transport", S11604-N16 "Atmospheres" and S11604-N16 "Stars". DB and EPL acknowledge also the Vienna Scientific Cluster (VSC project 70320) for computational resources. SE has been supported by the European Union Seventh Framework Program (FP7/2007-2013) under grant agreement no. 282703.

## References

- [1] Eggl, S., Pilat-Lohinger, E., Funk, B., Georgakarakos, N. and Haghighipour, N.: Circumstellar habitable zones of binary-star systems in the solar neighbourhood, MNRAS, 428:3104-3113, February 2013.
- [2] Haghighipour, N. and Raymond, S.: Habitable Planet Formation in Binary Planetary Systems, ApJ, 666:436-446, September 2007.

# Formation of embryos of the Earth-Moon system at the stage of rarefied condensations

**S. I. Ipatov** (1,2)

(1) Vernadsky Institute of Geochemistry and Analytical Chemistry of Russian Academy of Sciences, Moscow, Russia ([siipatov@hotmail.com](mailto:siipatov@hotmail.com)); (2) Space Research Institute of Russian Academy of Sciences, Moscow, Russia

## Abstract

The minimum value of the mass of the rarefied condensation that was a parent for the embryos of the Earth and the Moon could be about 0.02 of the Earth mass. There could be also another main collision of the parental condensation with another condensation, which changed the tilt of the Earth to its present value. Depending on eccentricities of planetesimals that collided with solid embryos of the Earth and the Moon, the Moon could acquire 0.04-0.3 of its mass at the stage of accumulation of solid bodies while the mass of the growing Earth increased by 10 times.

## 1. Introduction

Galimov and Krivtsov [1] noted that the giant impact concept, which is a popular model of the Moon formation, has several weaknesses. In particular, they calculated formation of the Earth-Moon system from a rarefied protoplanet. Lyra et al. [4] showed that in the vortices launched by the Rossby wave instability in the borders of the dead zone, the solids quickly achieve critical densities and undergo gravitational collapse into protoplanetary embryos in the mass range  $0.1-0.6M_E$  (where  $M_E$  is the mass of the Earth). Ipatov [2] and Nesvornyy et al. [5] supposed that transneptunian satellite systems have been formed from rarefied condensations. It was shown in [2] that the angular momenta acquired at collisions of condensations moved in circular heliocentric orbits could have the same values as the angular momenta of discovered transneptunian and asteroid binaries. Ipatov [3] obtained that the angular momenta used in [5] as initial data in calculations of the contraction of condensations leading to formation of transneptunian binaries could be acquired at collisions of two condensations moved in circular heliocentric orbits. I supposed that the number of collisions of condensations at which the formed condensation with

mass equal to that of a solid body with diameter  $d > 100$  km got the angular momentum needed for formation of a satellite system can be about or a little greater than the number of small bodies with  $d > 100$  km having satellites (among all such small bodies), i.e., the fraction of condensations formed at such collisions among all condensations can be about 0.3 for objects formed in the transneptunian belt. The model of collisions of condensations explains negative angular momenta of some observed binaries, as about 20 percent of collisions of condensations moving in circular heliocentric orbits lead to retrograde rotation.

## 2. The angular momentum at a collision of two rarefied embryos

Using the formulas presented in [2], we obtained the angular momentum of the Earth-Moon system could be acquired at a collision of two rarefied condensations with a total mass not smaller than  $0.1M_E$ . We suppose that solid proto-Earth and proto-Moon could be formed by contraction of a condensation (e.g., according to the models of contraction of a condensation presented in [1, 5]). In calculations of contraction of condensations (of mass  $m$  and radius  $r$  equal to 0.6 of the Hill radius) presented in [5], satellites were formed at initial angular velocities  $\omega_0$  from the range  $0.5\Omega_0-0.75\Omega_0$ , where  $\Omega_0 = (Gm/r^3)^{1/2}$  ( $G$  is the gravitational constant). In 3-D calculations of gravitational collapse of a condensation presented in [1], binaries were formed at  $\omega_0/\Omega_0$  from the range of 1-1.46. For smaller  $\omega_0/\Omega_0$ , satellites were not formed. At a collision of two condensations, the angular velocity can be as high as  $0.9\Omega_0$  [2]. Collided condensations could have some angular momenta before the collision. So in principle the resulting angular velocity of the formed condensation can exceed  $0.9\Omega_0$ . The difference in results presented in [1] and [5] can be caused, in

particular, by different chaotic velocities of particles/bodies constituting condensations and by different sizes of condensations. The radii of condensations in calculations presented in [1] were smaller (e.g. by about a factor of 40 than the Hill radii for the example presented on page 108 in [1]). Therefore any initial angular velocities considered in [1] can be reached after contraction of the condensation formed at a collision of condensations close to Hill spheres (the angular velocity of a compressed condensation of radius  $r_c$  formed from a condensation with the Hill radius  $r_H$  and the angular velocity  $\omega_H$ , equals  $\omega_{rc}=\omega_H(r_H/r_c)^2$  [2]). In principle, the angular momentum of the condensation needed for formation of the Earth-Moon system could be acquired by accumulation only of small objects, but for such model, the parental condensations of Venus and Mars could also get large angular momentum, which was enough for formation of large satellites.

### 3. Relative growth of solid embryos of the Earth and the Moon

Let us consider the model of the growth of the solid proto-Earth and proto-Moon to the present masses of the Earth and the Moon ( $M_E$  and  $0.0123M_E$ , respectively) by accumulation of smaller planetesimals for the case when the effective radii of proto-Earth and proto-Moon are proportional to  $r$  (where  $r$  is the radius of a considered embryo). Such proportionality can be considered for large enough eccentricities of planetesimals. In this case, based on  $dm_M/m_M=k\cdot(m_M/m_E)^{2/3}dm_E/m_E$  we can obtain  $r_{Mo}=m_{Mo}/M_E=[(0.0123^{-2/3}-k+k\cdot(m_{Eo}/M_E)^{-2/3})]^{-3/2}$ , where  $k=k_d^{-2/3}$ ,  $k_d$  is the ratio of the density of the growing Moon of mass  $m_M$  to that of the growing Earth of mass  $m_E$  ( $k_d=0.6$  for the present Earth and Moon),  $m_{Mo}$  and  $m_{Eo}$  are initial values of  $m_M$  and  $m_E$ . For  $r_{Eo}=m_{Eo}/M_E=0.1$ , we have  $r_{Mo}=0.0094$  at  $k=1$  and  $r_{Mo}=0.0086$  at  $k=0.6^{-2/3}$ . At these values of  $r_{Mo}$ , the ratio  $f_m=(0.0123-r_{Mo})/0.0123$  of the total mass of planetesimals that were accreted by the Moon at the stage of the solid body accumulation to the present mass of the Moon is 0.24 and 0.30, respectively. In this case for the growth of the mass of the Earth embryo by 10 times, the mass of the Moon embryo increased by a factor of 1.31 and 1.43, respectively.

If we consider that effective radii of the embryos are proportional to  $r^2$  (the case of small relative velocities of planetesimals), then integrating  $dm_M/m_M=$

$=k_2\cdot(m_M/m_E)^{4/3}dm_E/m_E$ , we can get  $r_{Mo2}=m_{Mo}/M_E=[(0.0123^{-4/3}-k_2+k_2\cdot(m_{Eo}/M_E)^{-4/3})]^{-3/4}$ , where  $k_2=k_d^{-1/3}$ . In the case of  $r_{Eo}=m_{Eo}/M_E=0.1$  we have  $r_{Mo}=0.01178$  at  $k_2=1$  and  $r_{Mo}=0.01170$  at  $k_2=0.6^{-1/3}$ , and  $f_m$  equals 0.042 or 0.049, respectively. In this case for the growth of the Earth embryo mass by 10 times, the Moon embryo mass increased by the factor of 1.044 and 1.051 at  $k_2=1$  and  $k_2=0.6^{-1/3}$ , respectively. In the above model depending on eccentricities of planetesimals, the Moon could acquire 0.04-0.3 of its mass at the stage of accumulation of solid bodies during the time when the mass of the growing Earth increased by a factor of ten. Probably, the condensations that contracted and formed the embryos of other terrestrial planets did not collide with massive condensations, and therefore they did not get a large enough angular momentum needed to form massive satellites.

The initial mass of the rarefied condensation that was a parent for the embryos of the Earth and the Moon could be relatively small ( $0.02M_E$  or even less) if we take into account the growth of the angular momentum of the embryos at the time when they accumulated planetesimals. In this case, the angular momentum of the Earth and the Moon that have grown from the embryos could be the same as that for the real Earth-Moon system. There could be also the second main collision of the parental condensation with another condensation, at which the radius of the Earth's embryo condensation was smaller than the semi-major axis of the orbit of the Moon's embryo. The second main collision (or a series of similar collisions) could change the tilt of the Earth to its present value.

### References

- [1] Galimov E.M., Krivtsov A.M.: Origin of the Moon. New concept. / De Gruyter. Berlin. 168 p., 2012.
- [2] Ipatov S.I.: Mon. Not. R. Astron. Soc., vol. 403, pp. 405-414, 2010.
- [3] Ipatov S.I.: In Proc. IAU Symp. No. 293 "Formation, detection, and characterization of extrasolar habitable planets", Cambridge University Press. pp. 285-288, 2014.
- [4] Lyra W., et al.: Astron. Astrophys., vol. 491, pp. L41-L44, 2008.
- [5] Nesvorny D., Youdin A.N., Richardson D.C.: Astron. J., vol. 140, pp. 785-793, 2010.



# Formation of giant planetary systems: effect of the eccentricity and inclination damping

S. Sotiriadis (1), A.-S. Libert (1), B. Bitsch (2) and A. Crida (3)

(1) naXys, Department of Mathematics, University of Namur, 8 Rempart de la Vierge, 5000 Namur, Belgium

(2) Lund Observatory, Department of Astronomy and Theoretical Physics, Lund University, 22100 Lund, Sweden

(3) University of Nice-Sophia Antipolis CNRS / Observatoire de la Côte d'Azur, Laboratoire Lagrange UMR 7293, Boulevard de l'Observatoire, BP4229, 06304 NICE cedex 4, France

## Abstract

Observational evidence (e.g. strong spin-orbit misalignment) shows that a study of the efficiency of the disc-induced migration on the formation of non-coplanar systems is essential. We follow the orbital evolution of three giant planets in the late stage of the gas disc and investigate the influence of the eccentricity and inclination damping due to planet-disc interactions, on the final configurations of the systems. Our n-body simulations use the damping formulae for eccentricity and inclination provided by the numerical hydrodynamic simulations of Bitsch et al. (2013). We present the results of  $\sim 10000$  numerical experiments, exploring different initial configurations, planetary mass ratios and disc masses. Special attention is given to the multiple resonance captures during the migration of the planets and the subsequent growth in eccentricity and inclination. Our simulations correctly reproduce the observed eccentricity distribution except for low initial disc masses. We also show that a significant fraction of non-coplanar systems are formed, despite the strong inclination damping.

## 1. Introduction

Several mechanisms have been invoked to explain the surprising variety of configurations of extrasolar systems, such as the high obliquities in respect to the orbital planes of some exoplanets and the eccentricity distribution of the observed ensemble. It seems that the interaction between the planets and their natal protoplanetary disc, at the early stage of formation, plays an important role for the sculpture of these systems. Resonant eccentricity and inclination excitation during the gas phase ([4], [8], [6]) and planet-planet scattering of unstable, initially coplanar, systems after the dispersal of the disc ([5], [7]) are some of the processes showing that planet-disc interactions play an important role in the diversity of planetary systems. The study of

the impact of a well modelled eccentricity and inclination damping on the final configurations of the giant planet systems is the goal of the present work.

## 2. Methods

We consider initially  $\sim 10000$  three-planet system embedded in a protoplanetary disc and evolving around a Solar-mass star. We study only systems with gas giant planets that have already formed their massive gaseous envelopes, and so they do not accrete any more material from the disc as they migrate inwards, towards the star. We use the symplectic integrator SyMBA ([3]), which allows us to handle close encounters between the bodies by employing a multiple time step technique. In order to mimic the interaction with the disc and to have a qualitative approach for the timescales of eccentricity and inclination damping, we use the formula provided by the hydrodynamical simulations of [1]. We use two different modelizations of the gas in the disc. In our first method, we introduce a constant-mass approximation for the circumstellar disc. We aim to study the potential establishment of different mean motion resonances and interpret, through statistical analysis, whether the inclination damping has a strong effect on the formation of these resonant configurations. For the second ensemble of simulations, we use a more "realistic" model for the evolution of the protoplanetary disc, decreasing its mass exponentially and setting the dispersal time at  $\sim 1 Myr$ . We stop the interaction with the disc when  $\dot{M}_{vis} < 10^{-9} M_{star}/yr$ . For both models, our parameter space contains different planetary mass ratios and disc masses. The initial surface density profile of the disc is  $\Sigma \propto r^{-0.5}$ .

## 3. Results

We observe a very good agreement between the population of systems obtained by our simulations and the detected one, especially for the eccentricities. In Figure 1, we show the cumulative distribution functions

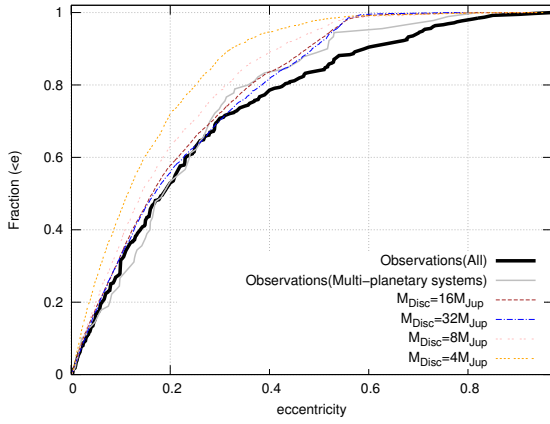


Figure 1: The cumulative distribution functions (CDF) of eccentricity for the observed population of planets with mass  $M_p \in [0.65, 10] M_{Jup}$  (black solid line), the detected planets in multi-planetary systems (grey solid line), and our simulated population considering different masses of the disc.

of the eccentricities for the confirmed giant planets with  $0.65 < M_p < 10 M_{Jup}$  (black solid line – the grey solid line refers to the subset of planets in multi-planetary systems) and the planets resulting from our simulations (four coloured dashed lines, corresponding to different initial mass of the disk). The curves are very similar, except for very low initial disk mass.

The efficiency of the migration mechanism is connected to the surrounding gas in the vicinity of the planet. Therefore, the final semi-major axis distribution depends on the initial mass of the disk and for the first ensemble of our simulations, in which we use a constant-mass model, we observe an overabundance of planets in small distances from the parent star. Nonetheless, removing the gas exponentially, we observe a good matching of our results with the semi-major axis distribution of the observed giant planet population.

Concerning the inclinations, most of the systems are found with small inclinations ( $< 10^\circ$ ) after the dispersal of the gas disk. Despite the fact that many systems enter an inclination-type resonance during the migration phase, the disc damps the inclination in a relatively short time-scale, leading the planets back to the midplane. Nevertheless, a significant fraction of the systems end-up with high mutual inclinations, even for initially massive disk.

Spin-orbit misalignments of Hot Jupiter planets are also observed in the simulated population. However,

most of the planets of the final one-planet systems are located in the midplane of the disc. This observation supports the work of [2], showing a possible disc-induced origin to the large fraction of aligned Hot Jupiters currently observed.

Finally, the different resonant configurations reached during the gas phase are investigated thoroughly, and the impact of the eccentricity and inclination damping on the resonance capture in low- and high- resonances is clearly identified.

## Acknowledgements

This work is part of the F.R.S.-FNRS "ExtraOr-DynHa" research project. This research used resources of the "Plateforme Technologique de Calcul Intensif (PTCI)" located at the University of Namur, Belgium, which is supported by the F.R.S.-FNRS.

## References

- [1] Bitsch, B., Crida, A., Libert, A.-S., and Lega, E.: Highly inclined and eccentric massive planets: I. planet-disc interactions, *Astronomy and Astrophysics*, vol. 555, pp. A124, 2013.
- [2] Crida, A., and Batygin, K.: Spin-orbit angle distribution and the origin of (mis)aligned hot Jupiters, *Astronomy and Astrophysics*, vol. 567, pp. A42, 2014
- [3] Duncan M., Levison, H., and Lee, M.: A multiple time step symplectic algorithm for integrating close encounters, *Astronomical Journal*, vol. 116, pp. 2067-2077, 1998
- [4] Lee, M. H., and Peale, S. J.: Dynamics and Origin of the 2:1 Orbital Resonances of the GJ 876 Planets, *Astrophysical Journal*, vol. 567, pp. 596-609, 2002.
- [5] Libert, A.-S., and Tsiganis, K.: Formation of '3d' multiplanet systems by dynamical disruption of multiple-resonance configurations, *Monthly Notices of the Royal Astronomical Society*, vol. 412, pp. 2353-2360, 2011.
- [6] Libert, A.-S., and Tsiganis, K.: Trapping in high-order orbital resonances and inclination excitation in extrasolar systems, *Monthly Notices of the Royal Astronomical Society*, vol. 400, pp. 1373-1382, 2009.
- [7] Matsumura, S., Thommes, E.W., Chatterjee, S., and Rasio, F.A.: Unstable Planetary Systems Emerging Out of Gas Disks. *Astrophysical Journal* 714, pp. 194-206, 2010
- [8] Thommes, E., and Lissauer, J.: Resonant inclination excitation of migrating giant planets, *Astrophysical Journal*, vol. 597, pp. 566-580, 2003.

# Possible new members of Datura asteroid family

A. Rosaev (1), E. Plavalova (2)

(1) NPC “Nedra”, Yaroslavl, Russia (hegem@mail.ru), (2) Astronomical Institute Slovak Academy of Science, Bratislava, Slovakia (plavalova@komplet.sk)

## Abstract

The problem of origin and age of asteroid families is studied very intensively. The youngest families are the most interesting due to the possibility to reconstruct their collisional history. Here we report about three possible new members of Datura family.

## 1. Method and Results

A search for new members of young asteroid families was done. The list of orbital elements of 415000 asteroids with permanent numbers and 200000 non-numbered asteroids was used. The method of selection of the nearest orbits is similar to that used in [1]. In some cases of the most recent events, the reconstruction of the origin of the asteroids in close orbits is possible in models of low-velocity breakup. In our results, three new members of Datura family (338309, 2002 RH291, 2014 OE206), not listed in [2, 3], were detected (table 1). The age of Datura family is estimated to be approximately  $450 \pm 50$  thousands years [2]. It means, that we can use osculating orbital elements for the study of this family.

Table 1: Osculating orbital elements of Datura family members at epoch 16-01-2009

Object	$\omega$	$\Omega$	$e$	$a$
1270 Datura	258.84072	97.881919	0.207917	2.234316
215619 2003 SQ168	259.39568	97.467904	0.207908	2.234266
60151 1999 UZ6	260.57151	96.799872	0.207812	2.235186
89309 2001 VN36	266.85629	92.976202	0.206341	2.235595
90265 2003 CL5	261.84375	95.697778	0.207471	2.234865
203370 2001 WY35	260.44606	96.872107	0.207435	2.235226
2003 UD112	263.12446	95.478778	0.206934	2.234566
<b>338309 2002 VR17</b>	260.60046	96.806362	0.207747	2.235169
<b>2002 RH291</b>	262.04302	95.759280	0.207613	2.235326
<b>2014 OE206</b>	261.72701	96.265302	0.206975	2.235606

The distribution of Datura family members in coordinates  $(a, e)$  is given in Fig.1 where new members are shown as a dots and the original members as a diamonds.

Numeric integration has shown that two of the new members of Datura family have recent close encounters with original members (table 2).

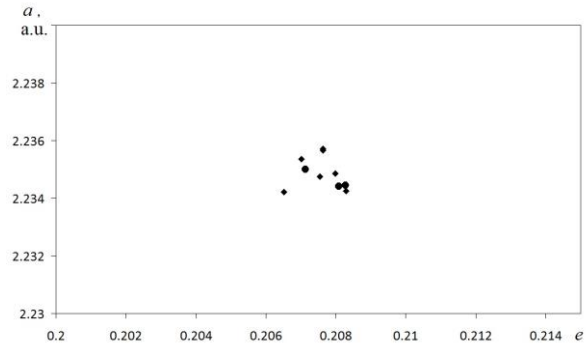


Figure 1: The positions of Datura family members in  $(a, e)$  coordinates

Table2. Recent close encounters in Datura family

#	Objects	Epoch	Distance, km
1	60151 2002RH	1844 Sept	25500
2	203370 2014OE	1875 Mar	126000

These new members can help to understand the circumstances of the origin of Datura family. For example, an important question to ask is if all the known members of Datura family have a common origin or if they came into existence in a few recent subsequent low-velocity breakups?

## 2. Summary and Conclusions

We have found three new members of Datura asteroid family. These new members can help provide us with a clearer understanding and more accurate estimation of the epoch and circumstances of the origin of Datura family.

## References

- [1] Nesvorný D., Vokrouhlický D. New candidates for recent asteroid breakups. The Astronomical Journal, 132, pp.1950-1958, (2006)
- [2] Nesvorný D., Vokrouhlický D., Bottke W.F.: The Breakup of a Main-Belt Asteroid 450 Thousand Years Ago, Science, 312, pp.1490, 2006

[3] Nesvorný D., Brož M., Carruba V.: Identification and Dynamical Properties of Asteroid Families  
arXiv:1502.01628v1 [astro-ph.EP] 5 Feb 2015

# Secular architecture of giant-planet dominated binary star systems

Á. Bazsó (1), E. Pilat-Lohinger (1), B. Funk (1) and S. Eggl (2)

(1) Institute for Astrophysics, University of Vienna, Austria; (2) IMCCE, Paris Observatory, France (bazso@astro.univie.ac.at)

## Abstract

We present a study on S-type planets in binary star systems with separations  $a < 100$  AU. For systems with at least one detected giant planet we determine the location of (linear) secular resonances with that planet by means of a semi-analytical method. We demonstrate that under some conditions, e.g. when the secondary star is at about 20 AU, the habitable zone can be perturbed or completely destabilized in these systems.

## 1. Introduction

Extra-solar planets are present also in binary and multiple star systems. There are currently 106 detected planets in 73 binary star systems, additionally also 20 planets in 15 multiple star systems are known (see Binary Catalogue of Exoplanets<sup>1</sup>). In the majority of binary star systems (56 out of 73) we find so called S-type planets. S-type planets orbit about one of the stars; whereas P-type planets orbit the whole binary in some distance [4].

Duquennoy & Mayor [3] have found for solar-type stars (spectral classes F7 – G9) that about 38% are members of binary star systems, and 5% are in multiple star systems (with three or more stars). Raghavan et al. [8] investigated exoplanet host stars and derived a lower limit of 21% for the fraction of binary star systems. In a more recent study Roell et al. [9] found only a multiplicity rate of 12% for exoplanet host stars.

Currently giant planets dominate the census of exoplanet in binary star systems. Planets with masses comparable to Earth's are missing or rare, a possible candidate is the planet of  $\alpha$  Centauri B [2]. We investigate the circumstances when additional terrestrial planets can be expected in binary star systems and whether these would be dynamically stable.

## 2. Systems

We selected 9 binary star systems with (projected) separations of the two stars below 100 AU, i.e. periods between  $10^4$  and  $10^6$  days [1].

Table 1: Selection of exoplanet-hosting binary star systems with giant planets. The systems are ordered according to their separation  $a_B$ ; the given mass ratio is calculated as  $M_B/(M_A + M_B)$ .

system	$a_B$ [AU]	mass ratio	planets
HD 19994	100	0.40	1
HD 177830	97	0.14	2
HD 1237	68	0.13	1
HD 120136	45	0.24	1
HD 41004	23	0.36	1
HD 128620	23	0.54	1
HD 196885	21	0.25	1
HD 222404	20	0.23	1
HD 13445	19	0.37	1

In these exoplanetary systems the giant planet can be either interior to the habitable zone or exterior to it. The secondary star can be expected to be on an eccentric orbit; after [3] the mean eccentricity is 0.3 for such separations. As a consequence perturbations from both the giant planet and the secondary star will affect the dynamics of potential terrestrial planets.

## 3. Methods

We investigated the secular dynamics of the terrestrial test planets (assumed to be massless objects) by applying a semi-analytical method [7]. We used the first-order Laplace-Lagrange secular theory [6] to calculate the secular frequencies of objects moving under the gravitational influence of two much more massive bodies. From a single numerical integration we can then determine the apsidal precession frequencies for the massive bodies with a Fourier analysis. Combin-

<sup>1</sup><http://www.univie.ac.at/adg/schwarz/multiple.html>

ing these calculated frequencies we determined the location of linear secular resonances and the regions of chaotic motion.

## 4. Results

Solar-system like combinations of a terrestrial planet interior to the giant planet's orbit may suffer from secular resonances; this is the case for at least three systems from our list, namely HD 41004, HD 196885, and HD 222404. The giant planet's eccentricity plays a crucial role for increasing the test planet's eccentricity. Even initially circular orbits may undergo eccentricity oscillations large enough to remove the planets partly or completely from the habitable zone, in some cases they are even removed from the system. The large eccentricities make it necessary to consider extended or average habitable zones [5].

Close-in giant planets in hot-Jupiter like orbits are generally less affected by the secondary star and have consequently much longer secular periods. However, the general relativistic precession of the pericenter introduces another effect that can increase the precession rate to values large enough to affect planets close to the habitable zone.

## 5. Conclusions

- Binary star systems with a giant planet can feature linear secular resonances close to or inside the habitable zone of the primary star.
- The giant planet's eccentricity induces a forced eccentricity on initially circular test planets and can lead to their ejection from the system.
- For close-in giant planets the relativistic precession of the pericenter needs to be taken into account when determining their precession frequency.

## Acknowledgements

This work was supported by the FWF projects P22603-N16 and NFN subproject S116-08 N16.

## References

- [1] Bazsó, Á., Pilat-Lohinger, E. and Eggl, S.: ApJ, in preparation, 2015.
- [2] Dumusque, X., Pepe, F., Lovis, C., et al.: An Earth-mass planet orbiting  $\alpha$  Centauri B, *Nature*, 491, pp. 207-211, 2012.
- [3] Duquennoy, A. and Mayor, M.: Multiplicity among solar-type stars in the solar neighbourhood. II - Distribution of the orbital elements in an unbiased sample, *A&A*, 248, pp. 485-524, 1991.
- [4] Dvorak, R.: Critical orbits in the elliptic restricted three-body problem, *A&A*, 167, 379-386, 1986.
- [5] Eggl, S., Pilat-Lohinger, E., Georgakarakos, N., et al.: An Analytic Method to Determine Habitable Zones for S-Type Planetary Orbits in Binary Star Systems, *ApJ*, 752, pp. 74-84, 2012.
- [6] Murray, C. D. and Dermott, S. F.: *Solar system dynamics*, Cambridge University Press, 1999.
- [7] Pilat-Lohinger, E., Bazsó, Á. and Funk, B.: *ApJ*, in preparation, 2015.
- [8] Raghavan, D., Henry, T. J., Mason, B. D., et al.: Two Suns in The Sky: Stellar Multiplicity in Exoplanet Systems, *ApJ*, 646, pp. 523-542, 2006.
- [9] Roell, T., Neuhäuser, R., Seifahrt, A. and Mugrauer, M.: Extrasolar planets in stellar multiple systems, *A&A*, 542, A92, 2012.

# Evolution of angular-momentum-losing exoplanetary systems

C. Damiani (1) and A.-F. Lanza (2)

(1) Institut d'Astrophysique Spatiale, UMR8617, Université Paris-Sud, Bâtiment 121, 91405 Orsay Cedex, France

(2) INAF - Osservatorio Astrofisico di Catania, Via Santa Sofia 78, 95123, Catania, Italy

## Abstract

We assess the importance of tidal evolution and its interplay with magnetic braking in the population of hot-Jupiter planetary systems. We show that the long-term evolution of planets orbiting F- and G-type stars is significantly different owing to the combined effect of magnetic braking and tides. Angular momentum loss has to be taken into account when constraining tidal evolution in close planetary systems.

## 1. Introduction

One of the long-standing problems in the field of exoplanets is understanding how short-period giant planets, usually called hot Jupiters, have reached their current orbit. According to the prevailing theory, giant planets must form beyond the snow line of a protoplanetary disk, which is typically located at a few astronomical units from the star. Hot Jupiters have a semi-major axis  $\lesssim 0.1$  AU, so they must have undergone some kind of migration.

Several migration theories are considered and they involve different halting mechanisms that can be tested by comparing their predictions with the observed orbital properties of exoplanets. However, further secular changes in the orbits of exoplanets can still be induced by tidal interaction between the planet and the star, even when the primordial migration mechanism is no longer effective. The tidal torque scales as the inverse of the sixth power of the semi-major axis  $a^{-6}$ , consequently it is especially important in the case of hot Jupiters. To test the migration scenarios, it is thus crucial to estimate the efficiency of tidal dissipation and its effects over the evolutionary lifetime of the star. But it is difficult to reach definite conclusions due to the limitations in our knowledge of the actual mechanism responsible for tidal dissipation, its efficiency, and the effects of angular momentum loss (AML) of the host through magnetic braking.

## 2. Magnetic braking and tides

Even without a detailed knowledge of the AML law or tidal dissipation mechanisms, there is a way to assess the general outcome of tidal evolution, using energy considerations only. Using the method of Lagrange multipliers we can characterise the minima of the total energy under the constraint that the total angular momentum shall be some unknown function of the stellar angular velocity only [2]. In this way we are considering that the total angular momentum of the star-planet system is not conserved, because magnetic braking exerts a torque on the star.

Thus we show that a stationary state can exist, and that it is characterized by circularity of the orbit, alignment between the spin of the planet, the star and the normal to the orbital plane, but not by co-rotation. The orbital mean motion of the planet at equilibrium is equal to the stellar angular velocity reduced by a factor  $\beta$  that depends on the AML rate through the stellar wind. The equilibrium is pseudo-stable if

$$\beta > 4 - \frac{1}{C_p + C_\star} \frac{M_\star M_p}{M_\star + M_p} a^2 \quad (1)$$

and

$$\beta > 0 \quad (2)$$

where  $a$  is the semi-major axis,  $C_p$  and  $C_\star$  are the moments of inertia of the planet and the star respectively and  $M_p$  and  $M_\star$  are their masses. This result is valid whatever the tidal dissipation mechanism may be and is independent of any tidal theory framework.

## 3. Characteristic time-scales

The resulting orbital evolution can be broken down into three limit regimes. They correspond to configurations in which the wind torque either dominates, is comparable to, or is dominated by, the tidal torque. We use a formulation of the tidal torque obtained in the framework of the equilibrium tide braking [1] assuming a constant  $Q' = 10^7$ . Magnetic braking is modelled with a Skumanich-type law and a torque



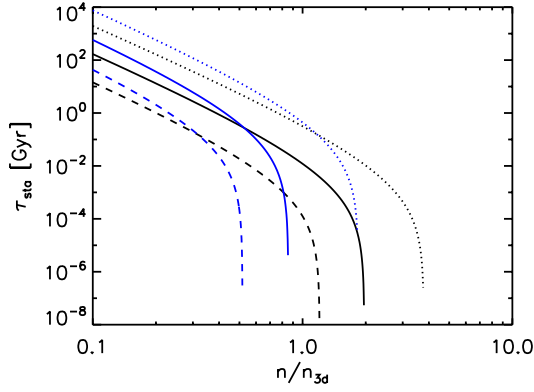


Figure 1: Estimates of the maximum possible duration of the stationary state as a function of the orbital mean motion in units of  $n_{3d} = 2\pi/(3\text{days})$ . The computations are done for a G-type star (black) or F-type star (blue) and planetary masses of 0.1 (dashed), 1 (solid), 10 (dotted) Jupiter masses.

of magnitude  $\Gamma_w = -\alpha_{mb} C_\star \Omega^3$ , where the value of  $\alpha_{mb}$  is estimated from observed rotational velocities of stars in clusters of different ages. We take  $\alpha_{mb} = 1.5 \times 10^{-14} \gamma \text{ yr}$  where  $\gamma = 1.0$  for G stars and  $\gamma = 0.1$  for F stars.

When the wind torque is much larger in amplitude than the tidal torque, we can consider that the stellar spin sets the pace of evolution. This is the case for typical stellar rotation rates of young stars and planets not closer than the 2:1 mean motion resonance. Depending on the initial rotation period of the star, this regime would last for about 50 My to 1 Gyr respectively for G-type stars (10 times longer for F-type stars).

When the wind torque is comparable to the tidal torque, the system can enter a stationary state where tidal evolution proceeds at almost constant stellar spin frequency, which allows to slow down the migration of the planet. A necessary condition for the establishment of the stationary state is that the tidal torque be opposite in sign and comparable in magnitude to the wind torque, and this can be maintained as long as there is enough orbital angular momentum compared to the stellar rotational angular momentum to maintain the torque balance. The duration of the stationary state as a function of the initial mean motion when a system enters into the stationary state is given in Fig. 1 for different stellar and planetary masses. Stars losing less angular momentum through their wind (F-type stars) can generally maintain the stationary state longer than

stars with a more efficient wind. For a given orbital distance, more massive planets can remain in the stationary state longer than less massive planets. In some cases, the stationary state can be maintained for a time-scale longer than the main-sequence lifetime of the star. For example, this would be the case of a Jupiter-sized planet entering the stationary state with an orbital period of 12-15 days.

When the tidal torque is much greater than the wind torque, tidal dissipation sets the characteristic time of in-spiral time  $\tau_a$ . This implies  $\tau_a \leq 100 \text{ Myr}$  for a Jupiter-mass planet and of the order of Myr for planets of more massive than  $5 M_J$ . There is thus a very low probability to observe massive planets in this phase of evolution. On the other hand, low-mass planets can have an in-spiral time that is longer than the main-sequence lifetime of their host star.

## 4. Summary and Conclusions

We have shown that when the magnetic braking of the star is considered, a tidal pseudo-stable equilibrium state can exist. For the known transiting exoplanets, we find that the distributions of angular momentum in systems with F and G-type stars display a statistically significant difference, and it is possible that most of the transiting planets in circular and aligned orbits be close to their stationary state. The distribution of angular momentum between the orbit and the stellar rotation gives information not only about the future evolution of a given system, but also on its possible initial angular momentum distribution at the beginning of binary tidal interaction. More detailed studies could help putting constraints on tidal dissipation efficiency, magnetic braking and migration scenarios.

## References

- [1] Barker, A. J. and Ogilvie, G. I.: On the tidal evolution of Hot Jupiters on inclined orbits, MNRAS, Vol. 395, pp. 2268-2287, 2009
- [2] Damiani, C. and Lanza, A. F.: Evolution of angular-momentum-losing exoplanetary systems. Revisiting Darwin stability, A&A, Vol. 574, pp.A39, 2015
- [3] Dobbs-Dixon, I., Lin, D. N. C., and Mardling, R. A.: Spin-Orbit Evolution of Short-Period Plane, ApJ, Vol. 610, pp. 464-476, 2004
- [4] Lanza, A. F., Damiani, C. and Gandolfi, D.: Constraining tidal dissipation in F-type main-sequence stars: the case of CoRoT-11, A&A, Vol. 529, pp. A50, 2011



# PRIME: Studying Low-Velocity Impacts in Microgravity

J. Colwell, J. Brisset, A. Dove, A. Whizin, H. Nagler and N. Brown

(1) Planetary Sciences Group, Department of Physics, University of Central Florida, 4000 Central Florida Blvd, Orlando FL 32816-2385, jec@ucf.edu

## Abstract

We report on the results of the third PRIME (Physics of Regolith Impacts in Microgravity Experiment) campaign on-board the NASA C-9 airplane in August 2014. The objective of the PRIME experiment is to study low-velocity impacts of cm-sized particles into dusty regolith under asteroid level- and microgravity conditions. First data analysis shows that this latest campaign successfully extended the previous measurements of coefficient of restitution and ejecta velocities to much lower impact energies.

## 1. Introduction

The dusty regolith of ring particles, proto-planetesimals, planetary satellites, and asteroids is subject to collisions at low velocities ( $v \sim 0.01$ -100 m/s) in addition to the hypervelocity ( $\geq 1$  km/s) impacts from the interplanetary micrometeoroid flux. In some regions of Saturn's rings, for example, the typical collision velocity inferred from observations by the Voyager spacecraft and dynamical modeling is a fraction of a centimeter per second [3]. These inter-particle collisions control the rate of energy dissipation in planetary rings and the rate of accretion in the early stages of planetesimal formation. Dust on the surface of planetary ring particles and small (1 cm – 10 m) planetesimals helps dissipate energy in the collision, but may also be knocked off, forming dust rings in the case of ring particles and slowing or inhibiting accretion in the case of planetesimals. Secondary impacts on asteroids and small planetary satellites occur at speeds comparable to the escape velocity from the object, or a few m/s for objects  $\sim 10$  km in radius or smaller. We report on impact experiments performed during the third PRIME campaign in the reduced-gravity environment of the NASA C-9 aircraft at speeds between 4 and 53 cm/s into simulated regolith.

## 2. The PRIME Experiment

The Physics of Regolith Impacts in Microgravity Experiment (PRIME) flies on the NASA C-9 and can perform impacts into granular materials at speeds of  $\sim 5$ -50 cm/s in microgravity. The experiment is conceptually identical to The COLLisions Into Dust Experiment (COLLIDE), which has flown on the space shuttle twice [1, 2] and has flown on the NASA KC-135 plane during two previous campaigns in 2002 and 2012 [2].

Impacts are performed in vacuum as ground-based experiments at 1g have consistently shown a strong effect of ambient air on the behavior of regolith in low-velocity impacts. Projectiles are spherical particles launched by a spring designed to provide the desired impact energy. The target materials studied in the work presented here are quartz sand and JSC-1 lunar regolith simulant, filled to a depth of 2 cm in the target tray. Projectile materials are quartz, brass, and stainless steel, providing a range of masses with the same projectile radius. Impacts are performed in isolated chambers (Figure 1) and up to 8 experiments can be performed per flight.

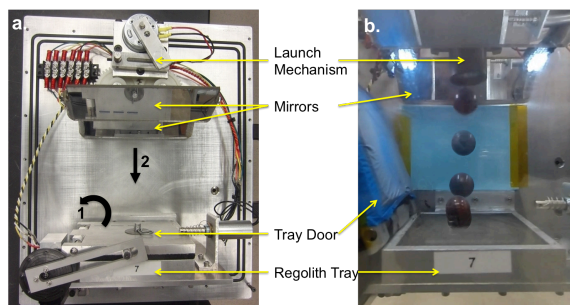


Figure 1: PRIME hardware inside the vacuum box. a. Before flight. Regolith is stored in the regolith tray that opens (1) to allow for the launched marble (2) to impact. The launch mechanism mainly consists of a spring, which constant, in coordination with the marble mass, determines the launch velocity. b. During flight. Montage of 7 recorded frames of a marble impact and rebound on a JSC-1 bed. The marble is much slower after impact.

The data collected consists of video recordings of the produced impacts, taken with a high-speed video camera at 120 frames per second. The camera views the impact with the line of sight parallel to the target surface and perpendicular to the projectile trajectory in the image plane (Figure 1.b). Two mirrors inside the impact chamber provide additional views of the impact (Figure 2.b).

### 3. Results and First Data Analysis

During the PRIME-3 flight campaign in August 2014, the experiment flew 4 times allowing for the recording of up to 8 impacts per flight. As asteroid gravity-level parabolas were flown during this campaign, 7 impacts were performed at 0.05g.

The successful impacts observed resulted in 9 marble rebounds and 15 impacts with ejecta (7 of which at 0.05g). Figure 2 shows an example of an impact into sand at 26 cm/s in microgravity.

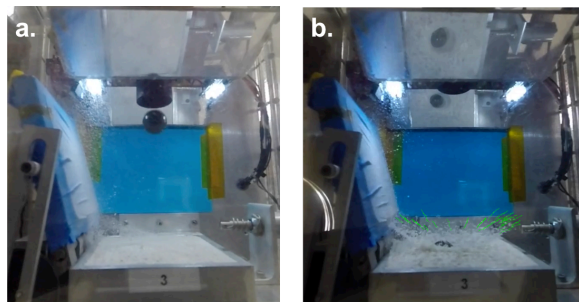


Figure 2: PRIME impact into sand in microgravity, a. just after marble launch, b. just after marble impact. The trajectories of manually tracked ejecta particles are shown in green.

For each rebound observed, the coefficient of restitution of the impact can be measured. Figure 3 shows that the PRIME-3 campaign successfully extended the region of the parameter field explored by investigating impacts at velocities lower than observed during the COLLIDE campaigns [1].

For each collision with ejecta, the highest number possible of individual ejected particles was tracked manually. For most of the impacts, the ejected particles had a normal velocity distribution. Figure 4 shows the mean ejecta velocities for the microgravity impacts compared to the former COLLIDE and PRIME campaigns. Here again, the PRIME-3 campaign successfully allowed for the exploration of much lower impact energies than in previous campaigns.

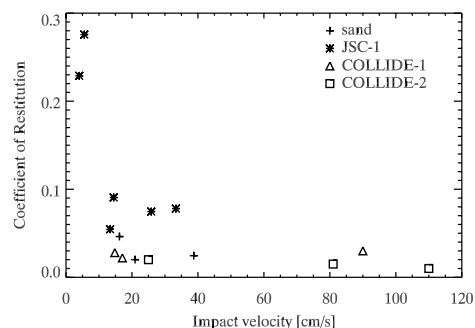


Figure 3: Coefficients of restitution of a marble on a bed of regolith measured during the PRIME-3 campaign. Data from the COLLIDE-1 and -2 campaigns is also shown [1].

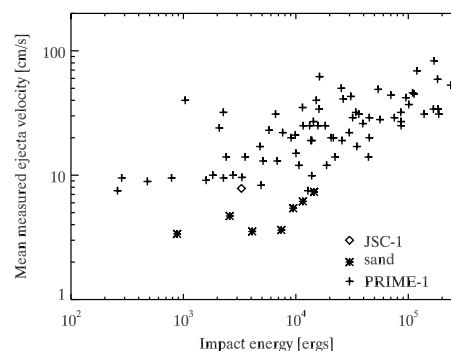


Figure 4: PRIME mean ejecta velocity in relation to the impact energy for microgravity impacts. Data from previous PRIME campaigns [2] is also shown.

### Acknowledgements

This material is based upon work supported by the National Aeronautics and Space Administration under grant NNX11AQ87G issued through the Planetary Geology and Geophysics Program and grant NNX09AB85G issued through the Origins of Solar Systems Program. We thank the NASA Flight Opportunities Program for providing the parabolic flight campaign and the NASA Reduced Gravity Office at Johnson Space Center for their invaluable support.

### References

- [1] Colwell, J. E., and Taylor, M. (1999) *Icarus* 138, 241-248.
- [2] Colwell, J. E. (2003) *Icarus* 164, 188-196
- [3] Esposito, L. W. (1993) *Annu. Rev. Earth Planet. Sci.* 21, 487-523.

# The fossil Oort cloud and the dynamics beyond Neptune

**M. Saillenfest** (1,2), M. Fouchard (1,3), G. Tommei (2), G. Valsecchi (4,5)

(1) IMCCE, Observatoire de Paris, (2) Dipartimento di Matematica, Università di Pisa, (3) LAL-IMCCE, Université de Lille, (4) IAPS-INAF, Roma, (5) IFAC-CNR, Sesto Fiorentino.

melaine.saillenfest@obspm.fr

## Abstract

We will present here some dynamical features of the so-called fossil Oort cloud (semi major axis between 100 and 1000 AU and perihelion beyond Neptune). This region has been considered so far as totally inert, because either the planetary perturbations or the galactic tides have an extremely weak effect. However, we will show that Kozai effect can still be efficient at very high distances from the planets, and result in high amplitude oscillations of the perihelion distance on a gigayear time-scale.

## 1 Introduction

The Oort cloud is a spherical reservoir of comets situated in the outermost confines of the Solar System (up to about  $10^5$  astronomical units from the Sun). Starting from the pioneer work of Oort, the cloud's dynamics is nowadays fairly well understood, mainly governed by galactic tides, passing stars and occasional close encounters with the planets. However, the internal limit of the Oort cloud is still very ill-defined, and particularly its junction with the inner Solar System (from about 100 to 1000 AU).

Contrary to the "classic" Oort cloud, this region is observable from the Earth: indeed, several bodies have been detected with extremely high perihelion distances (Sedna for instance). Furthermore, long-term simulations by M. Fouchard et al. [1] show that it is continually replenished by objects coming from the outer Oort cloud itself, which guarantees that the region is active. These aspects may be considered as hints for a surprisingly rich long-term dynamic.

## 2 Overview

Following the work of Kozai [3], Thomas and Morbidelli [4] or Gallardo et. al [2], we will present here

some numerical tools for the study of the fossil Oort cloud's dynamics, along with an analytical secular theory (the problem is reduced to a conserved Hamiltonian with two degrees of freedom). The figures below present some preliminary results: in particular, figure 3 illustrates the considerable effect of a high order mean motion resonance with Neptune (ratio 37:2).

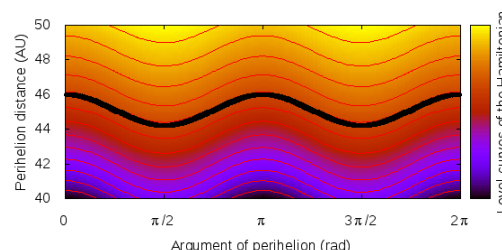


Figure 1: Secular theory vs. numerical integration – circulation case.

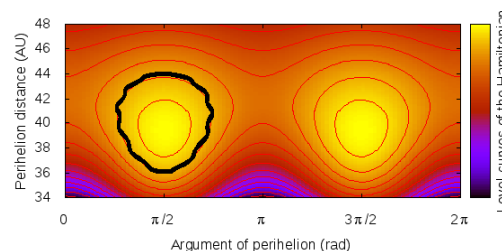


Figure 2: Secular theory vs. numerical integration – libration case.

## Acknowledgements

This work is conducted thanks to the advice of Andrea Milani and Giovanni Gronchi, from the Dipartimento di Matematica of Pisa. We thank them for their help.

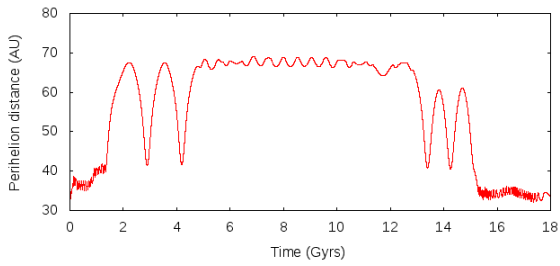


Figure 3: Kozai dynamics near a mean motion resonance with Neptune.

## References

- [1] M. Fouchard, H. Rickman, C. Froeschlé and G. Valsecchi: Planetary perturbations for Oort cloud comets III – Evolution of the cloud and production of centaurs and Halley type comets, *Icarus*, 2014.
- [2] T. Gallardo, G. Hugo, P. Pais, Survey of Kozai dynamics beyond Neptune, 2012.
- [3] Y. Kozai: Secular perturbations of asteroids with high inclination and eccentricity, *Astronomical Journal*, 1962.
- [4] F. Thomas and A Morbidelli: The Kozai Resonance in the Outer Solar System and the Dynamics of Long-Period Comets, *Celestial Mechanics and Dynamical Astronomy*, 1996.

# **Extreme, variable debris disks produced by giant impacts during terrestrial planet formation**

**Alan P. Jackson**

School of Earth and Space Exploration, Arizona State University, USA (alan.jackson@asu.edu)

## **Abstract**

Giant impacts between planetary scale bodies release large quantities of debris into their host systems. This debris, especially vapour condensates, may be extremely bright and optically thick. The variation in the shape of the dust cloud as it orbits the star, and undergoes Keplerian shear, can lead to large variations in the optical thickness, and consequent large variations in the observed flux, producing complex light-curves. By studying the light-curves of these extreme debris disks we can gain a powerful probe into the properties of the forming planets in the system.

## **1. Introduction**

Debris discs are traditionally taken to be low density, optically thin environments, however in the case of debris discs produced as the result of a giant impact between planetary scale bodies this may not be the case.

The collision of two planetary scale bodies is inherently a rather violent event. The material of the bodies will be subject to powerful shocks, which can be sufficient to vaporise the material. Even for a comparatively ‘gentle’ giant impact like the canonical Moon-forming scenario vaporises 10-30 per cent of the material (Canup, 2008).

Once material has been vaporised and launched into planetary or heliocentric orbit it will expand and cool, rapidly condensing into mm-cm scale droplets (Johnson & Melosh, 2012). One per cent of an Earth mass in mm-size particles has a total surface area of around  $3 \text{ AU}^2$  (absorbing area of  $0.75 \text{ AU}^2$ ). With such an enormous absorbing area it is clear that optical thickness will play a significant role.

We present a framework for the optical thickness of debris released in giant impact events and use simple models to discuss the observational effects on the resulting disks, particularly focusing on the appearance of variability in the very early stages. We discuss the application of our work to the newly discovered class of extreme (and variable) debris disks, as exemplified

by ID8 (Meng et al., 2014), and to the giant impact stripping of the Mercurian mantle, and illustrate how this can allow us to gain new insights into forming systems of terrestrial planets.

## **2. Modelling approach**

We adopt the formalism of Jackson et al. (2014) and describe the debris release in terms of the scaled velocity dispersion  $\sigma_v = \Delta v / v_k$ , where  $\Delta v$  is the (Gaussian) width of the velocity distribution, and  $v_k$  is the circular Keplerian speed at the collision-point. We expect  $\sigma_v$  to scale approximately as the escape velocity of the progenitor body (Leinhardt & Stewart, 2012, e.g.), and so  $\sigma_v$  can be used as a proxy for mass. Similarly the Keplerian speed is a proxy for orbital distance ( $v_k \propto a^{-1/2}$ ), and thus the behaviour of giant impact debris depends on both the mass of the progenitor and on the orbital distance at which the impact occurs.

To track the dynamics of the debris we use the Mercury  $N$ -body integrator (Chambers, 1999) with at least  $10^5$  particles per simulation. Since these  $N$ -body integrations are computationally expensive, using  $\sigma_v / v_k$  as the primary variable determining the dynamics of the debris allows us to explore a wider range of progenitor masses and orbital distances.

Optical thickness is tracked by assigning  $N$ -body particles a cross-sectional area and projecting them onto a surface to determine overlap between them.

## **3. Discussion**

There are two sources of optical thickness in observations of a debris disk, ‘internal’ and ‘line-of-sight’. Internal optical thickness is intrinsic to the disk and arises when the disk is optically thick to the light from the central star. Internal optical thickness will be higher if the debris is more spatially concentrated, either azimuthally in a clump or small arc, or vertically in a very thin structure. Line-of-sight optical thickness on the other hand arises as a result of our viewing geometry meaning that certain sight lines pass through

